WWW.IJRPR.COM

International Journal of Research Publication and Reviews

Journal homepage: www.ijrpr.com ISSN 2582-7421

Inelastic Scattering Across Single Josephson Junction

Chitra Prasad Lamichhane [a], Saddam Husain Dhobi [b,c]*

[a] Department of Physics, Prithvi Narayan Campus, Tribhuvan University, Nepal
[b] Central Department of Physics, Tribhuvan University, Kirtipur, Kathmandu, Nepal
[c] Innovative Ghar Nepal, Lalitpur, Nepal
DOI: https://doi.org/10.55248/gengpi.4.1123.113127

A B S T R A C T

This study investigates the differential cross section (DCS) across a single Josephson junction (SJJ) at high energy levels, employing the Kondo and Anderson models with impurities. A developed mathematical model yields the transition matrix, integrated with temperature derived from the Kondo and Anderson frameworks. Results reveal a decrease in DCS with rising photon energy and temperature, contrasting with an increase corresponding to the energy gap and repulsive energy. Notably, a comparative analysis demonstrates that the Anderson model consistently yields higher DCS values than the Kondo model. This exploration sheds light on the intricate interplay between impurities, temperature, and energy parameters in the context of SJJ, contributing valuable insights to the understanding of quantum phenomena in Josephson junctions.

Keywords: Differential cross section, single Josephson junction, Kondo and Anderson model, impurities, temperature and energy parameters

1. Introduction

The Kondo effect, discovered in 1934, revealed an unusual resistivity behavior in gold at low temperatures, attributed to impurities with magnetic moments, such as iron atoms. J. Kondo explained this using perturbation theory, coining the term "Kondo temperature" (T_K). However, his solution faced issues at zero temperature, leading to the Kondo problem. Subsequent renormalization group approaches, notably K. G. Wilson's numerical renormalization group in 1975, effectively addressed this problem (Hanl, 2014). Despite its resolution, the Kondo effect regained significance with nanotechnology advancements. Multiple methods exist for deriving the low energy scale T_K, with varying results due to its crossover nature. The poor man scaling approach offers valuable insights into how coupling is renormalized at lower energy scales (van der Wiel et al., 2000). The current study employs a Hubbard-Stratonovich treatment of Coulomb interactions on Quantum Dots (QDs), relying on auxiliary fields, with precision achieved through the path integral. However, the mean-field approximation adopted prohibits access to the Kondo regime for $T_K>\Delta$. For a Josephson junction (JJ) with a single QD, the T_K is determined by Haldane's formula, reaching at most $T_K = 0.13\Delta$, where Δ is an energy gap, in our numerical investigation. Past studies on the Kondo regime in a single Josephson junction involved either a Hubbard-Stratonovich transformation followed by Monte Carlo numerical treatment or an exact numerical renormalization group approach. Future work on double Josephson junctions could follow these approaches. If $T_K > \Delta$, the Kondo regime could be circumvented by adjusting QD gate voltages to favor specific phase combinations, as shown to enhance splitting efficiency (Jacquet, 2018).

JJs are pivotal for advancing quantum magnetic sensors and superconducting electronics. The discovery of iron-based superconductors has opened up the prospect of creating high-temperature JJs with minimal susceptibility to lattice irregularities near the barrier. This potential resilience stands out compared to ceramic superconductors, where junctions exhibit considerable scattering in electrical parameters due to anisotropic symmetry in the order parameter. To ensure practical viability, it is imperative to establish reliable technologies guaranteeing favorable values for critical current, normal resistance, and electrical capacitance, as emphasized (Sarnelli et al., 2014). The DCS analysis focuses on lower and higher frequencies, revealing a linear increase at lower frequencies and an exponential rise with fluctuations at higher frequencies. This study provides insights into scattering phenomena in superconductors with Kondo impurities, emphasizing the interplay between the Kondo effect, impurity scattering, and Josephson coupling. However, the authors do not investigate single Josephson junctions and the Anderson model. This research includes a single Josephson junction and Anderson model (Chaudhary et al., 2023). From the literature, it is observed that there is a notable research gap regarding the investigation of the DCS across an SJJ in the presence of impurities. While the work mentions a mean-field approximation and provides the T_K for a JJ containing a single QD, it does not delve into the specific implications of impurities on the DCS. Understanding the interplay between impurities and the DCS is crucial, especially in quantum computing and applications where information preservation is vital. The research gap highlights the need for a detailed exploration of how impurities influence the quantum behavior of JJs, shedding light on potential energy loss mechanisms and paving the way for advancements in preserving quantum information. Addressing this gap can contribute significantly to the understanding and optimization of Josephson junctions for various quantum-related applications.

SJJs are integral components in diverse applications, particularly in the realms of quantum computing, superconducting electronics, quantum metrology, and quantum information processing. In quantum computing, JJs serve as key elements in various qubit designs, facilitating quantum operations. Superconducting electronics leverage the unique properties of JJs, such as zero dissipation, for applications like analog-to-digital converters and ultra-sensitive magnetometers. In quantum metrology, these junctions enable the development of highly sensitive detectors for precise measurements of electromagnetic fields. Additionally, JJs play a crucial role in quantum information processing, contributing to the creation of qubits and advancing quantum communication and cryptography. The applications underscore the versatility and significance of SJJs across different domains of emerging technologies.

Nomenclature

DCS: Differential cross section

SJJ: Single Josephson Junction

T_K: Kondo Temperature

QDs: Quantum Dots

SIS: Superconductor-Insulator-Superconductor

SNS: Superconductor-Normal-Superconductor

JJ: Josephson Junction

2. Materials and Methods

Josephson junction consists of two superconductors coupled by a weak link. There are two types of Josephson junctions (i) Superconductor-Insulator-Superconductor (SIS) junction and (ii) Superconductor-Normal-Superconductor (SNS) junction. SIS junctions are also known as tunneling junctions because tunneling of cooper pairs takes place from one superconductor to the other through the insulator barrier. In the case of SNS junctions, there is no insulator barrier, there are only two SN interfaces. For the SJJ there exists another set of variables defined as

$$\begin{cases} \boldsymbol{K = n_1 + n_2} \\ \boldsymbol{k = \frac{1}{2}(n_2 - n_1)} \end{cases} \textbf{and} \quad \begin{cases} \boldsymbol{\Delta = \frac{1}{2}(\phi_1 + \phi_2)} \\ \boldsymbol{\delta = (\phi_2 - \phi_1)} \end{cases} \qquad (\mathbf{1})$$

The formula uses K to denote the total number of Cooper pairs while k denotes the difference in Cooper pairs between electrodes. The phase difference across the Josephson junction (δ) and the average phase Δ are conjugate variables to n and N. The Hamiltonian for the circuit is described in detail by (Agren, 2002).

$$\boldsymbol{H(\vec{n}, \vec{\varphi}) = \frac{(2e)^2}{2}\vec{n}^T C^{-1}\vec{n} + U(\vec{\phi})} \qquad (\mathbf{2})$$

Where $\boldsymbol{\vec{n}^T = [n_1, n_2]}$, $\boldsymbol{U(\vec{\phi}) = -E_J \cos(\phi_2 - \phi_1)}$, $\boldsymbol{E_J = \frac{\Phi_0 I_c}{2\pi} = \frac{h}{2e}\frac{1}{2\pi}\frac{\pi\Delta_0}{2eR_N}\tanh\left(\frac{\Delta_0}{2k_BT}\right)}$ and $\boldsymbol{C = \begin{bmatrix} C + C_0 & -C \\ -C & C + C_0 \end{bmatrix}}$ is Capacitance matrix. The Hamiltonian from (2) also can be written more general with K zero as

$$\boldsymbol{H(k, \delta) = 4E_{C\Sigma}k^2 - E_J cos\delta} \qquad (\mathbf{3})$$

Where $\boldsymbol{E_{C\Sigma} = \frac{e^2}{2C + C_0}}$ is an effective charging energy of JJ including the stray capacitance C_0. The Hamiltonian of noninteracting spin-1/2 fermions is derived by Goldstein et al. in 2013 as,

$$\boldsymbol{\hat{H}_K = \sum_{k,\sigma=\uparrow,\downarrow} vkc^{\dagger}_{k,\sigma}c_{k,\sigma} + \frac{I_z S_z}{2L}\sum_{k,\sigma,k',\sigma'} c^{\dagger}_{k,\sigma}\tau^z_{\sigma,\sigma'}c_{k',\sigma'} + \frac{I_{xy}S_-}{4L}\sum_{k,\sigma,k',\sigma'} c^{\dagger}_{k,\sigma}\tau^{+}_{\sigma,\sigma'}c_{k',\sigma'} + H.c - B_z S_z} \qquad (\mathbf{4})$$

Where $\boldsymbol{\tau^i_{\sigma,\sigma'}}$ is pauli matrices, $\boldsymbol{I_z = 2\pi v\left(1 - \frac{\alpha}{\sqrt{2}}\right)}$, and $\boldsymbol{I_{xy} = 2\pi a E_J^{LR}}$.Incoming microwave photons scatter elastically and inelastically due to the quantum impurity. $\boldsymbol{c}$ value for magnetic field applied. In equation (7) of Goldstein et al. (2013), all components of the elastic $\boldsymbol{\hat{T}}$matrix and the local dynamic differential spin susceptibility of the Kondo problem are described in further depth. The coupling parameter and the parameters ($\boldsymbol{\alpha_{\{L,R\}}}$) are provided by $\boldsymbol{\alpha_L = \alpha_R = \frac{1}{g}(1 - \lambda_{LR})}$, $\boldsymbol{\alpha^2 = \alpha_L^2 + \alpha_R^2}$ and $\boldsymbol{\lambda_{LR} = \frac{C_L C_R}{(C_L + C_R)C_{LR}} \sim \sqrt{\frac{C_g}{C}} \ll 1}$ (Goldstein et al., 2013). At high frequencies,$\boldsymbol{\omega \gg T_K}$,the arbitrary susceptibility is approaches (Hewson, 1993) as,

$$\boldsymbol{\chi_{zz}(\omega) = i\frac{\pi}{4}\frac{f(\alpha)}{\omega}\left(\frac{T_K}{i\omega}\right)^{2-\alpha^2}, \alpha > 1} \qquad (\mathbf{5})$$

Where $\boldsymbol{f(\alpha) = -2\sin\left(\frac{\pi\alpha^2}{2}\right)\frac{\Gamma(1-\alpha^2)}{\{\pi[c(\alpha)]^{2-\alpha^2}\}}}$. The array is uniform outside of the quantum impurity: all Josephson couplings, with the exception of the islands of the quantum impurity, are $\boldsymbol{E_J}$, and all capacitances to the ground and junction capacitances, respectively, are $\boldsymbol{C_g}$ and C. The scattering cross-section in terms of the transition matrix according to Bransden & Joachain and Sakurai using Kroll Watson Approximation (Kim, 2022) is given by

$$\frac{d\sigma}{d\Omega} = \frac{k_f}{k_i}\left(\frac{m^*(2\pi)^2}{\hbar^2}\right)^2 |T_{fi}|^2 \quad (6)$$

Where T is transition matrix m is mass of coopers pair $m^* = 2m$ and k_f and k_i is final and initial momentum of cooper pairs.On substituting the value from equation (5) in (6) and solving for $\ell = \ell'$ and $\ell \neq \ell'$

$$\frac{d\sigma}{d\Omega} = \frac{k_f}{k_i}\frac{16m^2\pi^4}{\hbar^4}\left|\omega\left(\frac{1}{g}(1-\lambda_{LR})\right)^2 \chi_{zz}(\omega)\right|^2 \quad (7)$$

Also using $\alpha^2 = 2$ and $g = 1$, $\lambda_{LR} \ll 1$, when $I_{xy} = I_z$, the DCS is For higher frequency $\omega \gg T_K$, from (7) and (5) with $\alpha \geq 1$, $T_K = c(\alpha)\omega_0\left(\frac{I_{xy}}{2\pi\alpha\omega_0}\right)^{\frac{2}{2-\alpha^2}}$, $c(\alpha)\sim 1$ is (photon of frequency ω incoming) obtained as for kondo model

$$\frac{d\sigma}{d\Omega} = \frac{k_f}{k_i}\left(\frac{m(2\pi)^3}{(2\pi)\hbar^2}\right)^2 \left|(1-\lambda_{LR})^2\frac{1}{16}\left(2\sin\left(\frac{\pi\alpha^2}{2}\right)\frac{\Gamma(1-\alpha^2)}{\{\pi[1]^{2-\alpha^2}\}}\right)\frac{I_{xy}^2}{\pi\alpha^2\omega\omega_0}\right|^2 \quad (8)$$

Since we have, $I_{xy} = 2\pi a E_J^{LR}$

$$\frac{d\sigma}{d\Omega} = \frac{k_f}{k_i}\left(\frac{m(2\pi)^3}{(2\pi)\hbar^2}\right)^2 \left|(1-\lambda_{LR})^2\frac{1}{16}\left(2\sin\left(\frac{\pi\alpha^2}{2}\right)\frac{\Gamma(1-\alpha^2)}{\{\pi[1]^{2-\alpha^2}\}}\right)\frac{\left(2\pi a E_J^{LR}\right)^2}{\pi\alpha^2\omega\omega_0}\right|^2 \quad (9)$$

For SJJ we have $E_J = E_J^{LR} = \frac{\Phi_0 I_c}{2\pi} = \frac{h}{2e}\frac{1}{2\pi}\frac{\pi\Delta_0}{2eR_N}\tanh\left(\frac{\Delta_0}{2k_BT}\right)$, then equation (9) become

$$\frac{d\sigma}{d\Omega} = \frac{4m^2\pi^4 k_f}{\hbar^4 k_i}\left|(1-\lambda_{LR})^2\left(\frac{\pi a^2}{\alpha^2\omega\omega_0}\right)\sin\left(\frac{\pi\alpha^2}{2}\right)\left(\frac{\Gamma(1-\alpha^2)}{\left[\frac{1}{2}\right]^{2-\alpha^2}}\right)\left(\frac{h\Delta_0}{6e^2R_N}\tanh\left(\frac{\Delta_0}{2k_BT}\right)\right)^2\right|^2 \quad (10)$$

This is equation for high frequency for SJJ. $(1-\lambda_{LR})^2$ this term represents the influence of Kondo impurities. It reflects the scattering behavior associated with the presence of these impurities. $\left(\frac{\pi a^2}{\alpha^2\omega\omega_0}\right)$ this term represent involvements of characteristic length (a), the dimensionless parameter (α), and frequencies (ω and ω_0). Describes the spatial and frequency characteristics of the scattering. $\sin\left(\frac{\pi\alpha^2}{2}\right)$ this term includes the sine of a term related to the dimensionless parameter α. Introduces a sinusoidal dependence, indicating a periodic behavior. $\left(\frac{\Gamma(1-\alpha^2)}{\left[\frac{1}{2}\right]^{2-\alpha^2}}\right)$ this term incorporates the gamma function (Γ) and further emphasizes the role of α in shaping the scattering process. $\left(\frac{h\Delta_0}{6e^2R_N}\tanh\left(\frac{\Delta_0}{2k_BT}\right)\right)^2$ this term describes the impact of superconductivity and temperature on the scattering. Understanding the detailed physical significance of each term requires knowledge of the specific system under consideration and the context of the scattering phenomenon with Kondo impurities. Additionally, the periodic and exponential components in the equation indicate complex and rich behavior in the scattering process, influenced by both fundamental constants and specific system parameters. Also for higher frequency $\omega \gg T_K$, from (7) and (5) with $\alpha \geq 1$, for Anderson model, $T_K = \sqrt{\frac{\Gamma U}{2}}\, e^{\pi\varepsilon_d(\varepsilon_d+U)/2\Gamma}$ (Choi et al., 2004). U= Coulomb repulsion between the dot electrons, where Γ corresponds to the width of the dot energy level due to hybridization with the reservoir, $\varepsilon_d = -\frac{U}{2}$, we have

$$\frac{d\sigma}{d\Omega} = \frac{4m^2\pi^6 k_f}{\hbar^4 k_i}\left|(1-\lambda_{LR})^2\left(\sin\left(\frac{\pi\alpha^2}{2}\right)\frac{\Gamma(1-\alpha^2)}{\left\{\left[\frac{1}{2}\right]^{2-\alpha^2}\right\}}\right)\left(\frac{\sqrt{\frac{\Gamma U}{2}}\, e^{\pi\varepsilon_d(\varepsilon_d+U)/2\Gamma}}{\omega}\right)\right|^2 \quad (11)$$

3. Results and Discussion

3.1 Kondo Model at high energy with impurities

This investigation focuses on the DCS behaviour across a SJJ at high energy levels, employing the Kondo model with impurities. The results, depicted in Fig. 1(a), showcase a noteworthy trend: the DCS exhibits a decrease with both photon energy and temperature, while concurrently increasing with the energy across the junction, as illustrated in Fig. 1(b). The Fig's. are constructed based on equation (10) within the Kondo model, emphasizing the significance of impurities in this high-energy context. In the SJJ, as electrons traverse the junction, elastic scattering occurs with varying photon energies. Remarkably, the observation reveals that at lower photon energies, the DCS is higher in the UV-Visible range but decreases in higher energy regions. This phenomenon is attributed to the intricate interaction between the target cooper pair across the junction and the incident photon energy. The results contribute valuable insights into the nuanced dynamics of DCS in the presence of impurities and high-energy conditions within a Josephson junction.

This study delves into the intricate dynamics of the DCS across a SJJ at high energy levels, incorporating insights from the Kondo model with impurities. Fig. 1(a) and Fig. 1(b) illustrate the behaviour of DCS, highlighting a dual impact of temperature on its variation across the SJJ. As temperature increases, a discernible decrease in DCS is observed, elucidating a nuanced relationship. In the lower temperature range, the DCS exhibits a higher value. This phenomenon is attributed to the shortened cooper pair bond under lower temperatures. As temperature rises, cooper pair electrons experience an increase in distance, resulting in reduced DCS. The intricate nature of this relationship stems from the diminishing interaction between cooper pair electrons and

incident particles as the temperature rises. Beyond a critical temperature, the cooper pairs undergo breakage, rendering the determination of DCS across the SJJ highly complex. The interplay between temperature, cooper pair dynamics, and DCS in the SJJ presents a multifaceted scenario. Lower temperatures foster a more favourable environment for cooper pair interactions, leading to higher DCS, while higher temperatures disrupt these interactions, resulting in a decrease in DCS. The critical temperature threshold introduces an additional layer of complexity, marking a transition point where cooper pairs break, challenging the straightforward determination of DCS. This comprehensive analysis underscores the intricate relationship between temperature and DCS, providing valuable insights into the behaviour of Josephson junctions in high-energy environments.

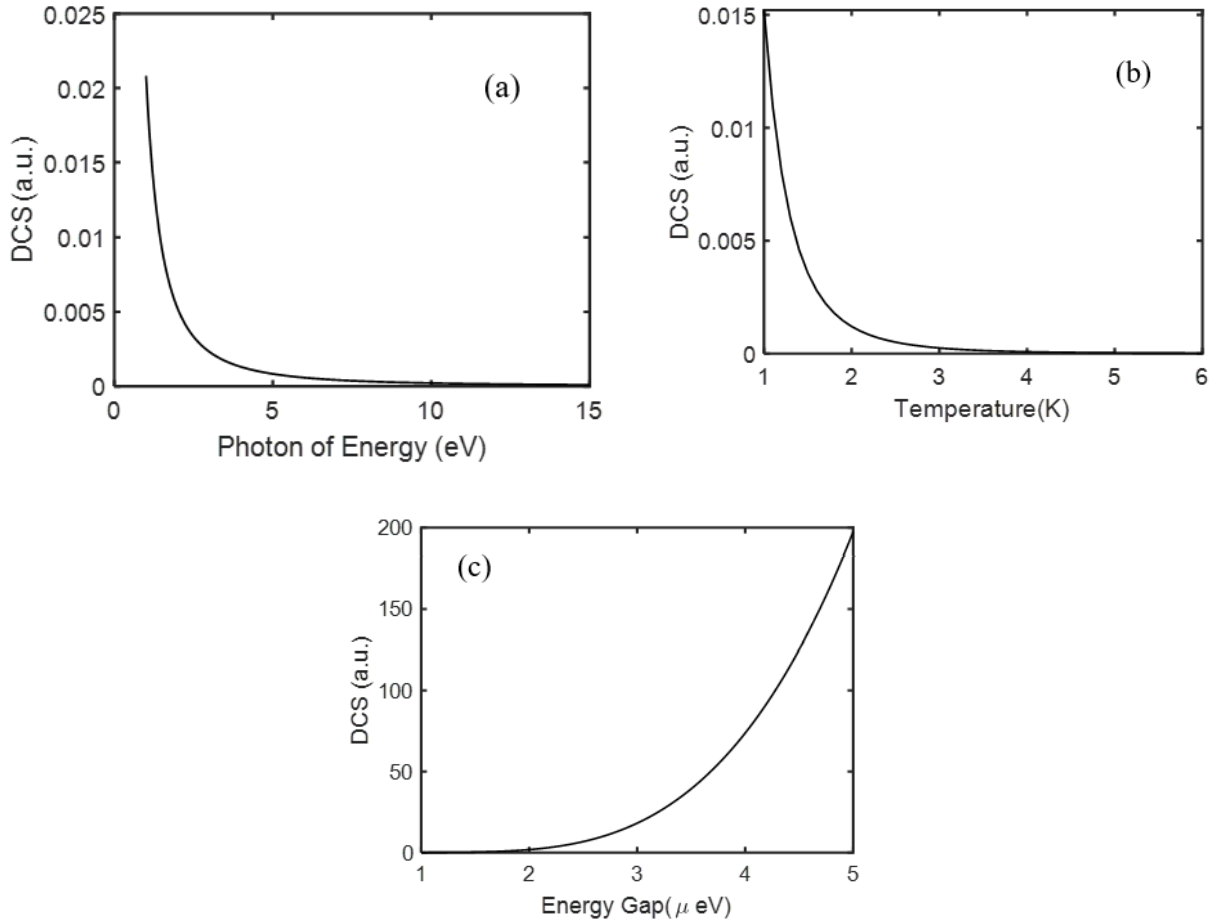

Fig. 1: DCS for Anderson model

The DCS across a SJJ at high energy levels, employing the Kondo model with impurities, reveals a noteworthy relationship between the DCS and the energy gap of superconductors, as depicted in Fig. 1(c). The Fig. illustrates a clear increase in DCS with the rising energy gap of superconductors. The observed phenomenon of lower DCS for a lower energy gap can be attributed to the heightened interaction of conduction/valence electrons in the superconducting state with incident electrons. The proximity of energy levels facilitates stronger interactions, resulting in a lower DCS. This is evident in the lower energy range where the energy gap is narrower, allowing for increased interactions. Conversely, as the energy gap of superconductors increases, the DCS experiences a significant upturn. The rationale behind this lies in the higher energy gap between the conduction/valence bands of superconductors and incident electrons. The larger energy gap provides a more favourable environment for interactions, leading to an augmented DCS. This is particularly pronounced in the higher energy range, where the increased energy gap allows for more effective coupling between the superconducting state and incident electrons. This intricate interplay between the energy gap of superconductors and the resulting DCS offers valuable insights into the quantum behaviour of Josephson junctions. The observed trends provide a nuanced understanding of how the energy gap influences the interaction dynamics, shedding light on the complex nature of high-energy phenomena in superconducting systems.

3.2 Anderson model at high energy with impurities

The behaviour of the DCS across a SJJ at high energy, employing the Anderson model and comparing it with the Kondo model. The results, presented in Fig. 2(a), delineate a notable trend: the DCS exhibits a decrease with both photon energy and temperature, while concurrently increasing with the energy across the junction. The observation reveals a nuanced relationship between photon energy and DCS, with higher values observed in the UV-Visible range for lower photon energies, contrasting with lower DCS in the higher energy region. This phenomenon is attributed to the heightened interaction between the target cooper pair across the junction and incident photons. The intricate interplay of photon energy and the cooper pair across the SJJ underscores the quantum nature of the system, influencing the DCS in a distinctive manner. Furthermore, a noteworthy comparison between the Anderson

and Kondo models is drawn, with the DCS for the Anderson model consistently exceeding that of the Kondo model. This comparison is grounded in the mathematical formulation encapsulated by equation (11), highlighting the distinct characteristics and predictive power of the Anderson model in elucidating the quantum behaviour of the SJJ at high energies.

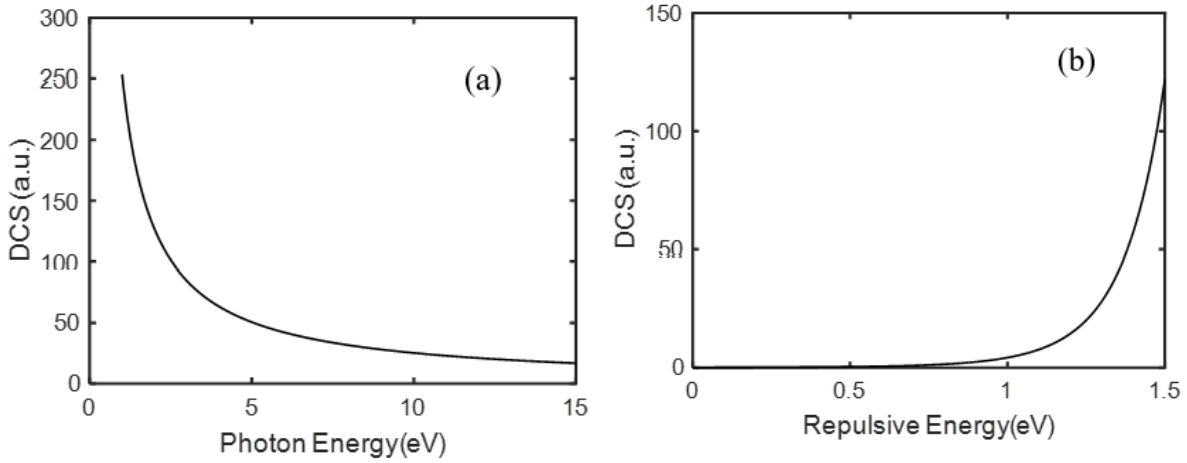

Fig. 2: DCS for Anderson model

The impact of repulsive energy on the DCS across a SJJ, providing insightful observations illustrated in Fig. 2(b). The results manifest a clear and significant increase in DCS with the varying levels of repulsive energy across the SJJ. The observed trend can be rationalized by considering the role of repulsive energy in separating the projectile and target entities across the junction. When repulsive energy is lower, the interaction between these entities is less hindered, resulting in a lower DCS. Conversely, higher levels of repulsive energy lead to an increased separation between the projectile and target, fostering a more favourable environment for interaction, thereby yielding a higher DCS. This behaviour can be intuitively understood by recognizing that repulsive energy acts as a barrier, influencing the distance between the interacting components. Lower repulsive energy allows for closer proximity, limiting the effectiveness of interactions, and consequently resulting in a lower DCS. Conversely, higher repulsive energy promotes a greater spatial separation, facilitating more effective interactions and, in turn, an elevated DCS.

4. Conclusion

In conclusion, this comprehensive investigation explores the DCS dynamics across a SJJ at high energy levels. In the Kondo model, DCS demonstrates a noteworthy decrease with increasing photon energy and temperature, concurrently rising with the energy across the junction. The interplay of temperature, cooper pair dynamics, and DCS reveals a multifaceted scenario, with lower temperatures fostering higher DCS and critical temperatures introducing complexity due to cooper pair breakage. Transitioning to the Anderson model, the DCS exhibits a nuanced relationship with photon energy, and a notable comparison with the Kondo model reveals consistently higher DCS values. Additionally, the impact of repulsive energy on DCS across the SJJ underscores its pivotal role in modulating interaction dynamics, providing valuable insights into the quantum behaviour of these systems.

Acknowledgements

The authors express their gratitude to the faculty members at Innovative Ghar Nepal for generously providing research space. Additionally, they would like to extend their appreciation to the faculty at the Department of Physics, Prithvi Narayan Campus, and the Central Department of Physics, Tribhuvan University, Nepal, for their motivation and insightful discussions pertaining to this study.

References

Agren, P. (2002). Charging effects in small capacitance Josephson junction circuits (Doctoral dissertation, Royal Institute of Technology, Department of Physics, Section of Nanostructure Physics).

Choi, M.-S., Lee, M., Kang, K., & Belzig, W. (2004). Kondo effect and Josephson current through a quantum dot between two superconductors. Physical Review B, 70(2), 020502. doi:10.1103/physrevb.70.020502

Goldstein, M., Devoret, M. H., Houzet, M., & Glazman, L. I. (2013). Phys. Rev. Lett., 110.

Haldane, F. D. M. (1978). Scaling theory of the asymmetric Anderson model. Phys. Rev. Lett., 40, 416–419.

Hewson, A. C. (1993). The Kondo Problem to Heavy Fermions. Cambridge University Press, Cambridge, England.

Jacquet, R. (2018). Josephson effects and Cooper pair splitting in modern hybrid devices. Superconductivity [cond-mat.supr-con]. Aix-Marseille Université. ffNNT : ff. fftel-02960668.

Kim, B. N. (2022). Angular Distribution of Electron-Helium Scattering in the Presence of a 1.17 eV Laser Field. Theses and Dissertations--Physics and Astronomy, 95.

Sarnelli, E., Adamo, M., Nappi, C., Braccini, V., Kawale, S., Bellingeri, E., & Ferdeghini, C. (2014). Scattering theory of the Josephson effect in iron-based superconductors. Applied Physics Letters, 104(16), 162601. doi:10.1063/1.4872218

Van der Wiel, W. G., De Franceschi, S., Fujisawa, T., Elzerman, J. M., Tarucha, S., & Kouwenhoven, L. P. (2000). The Kondo Effect in the Unitary Limit. Science, 289(5487), 2105–2108. doi:10.1126/science.289.5487.2105

Hanl, M. J. (2014). Optical and transport properties of quantum impurity models – an NRG study of generic models and real physical systems. Dissertation an der Fakultät für Physik der Ludwig–Maximilians–Universität München.

Chaudhary, S., Gupta, S. P., Nakarmi, J. J., Yadav, K., Dhobi, S. H. (2023). Quantifying the effect of temperature on differential cross-section in Josephson-junction systems. Hadronic Journal, 46, 249–262. doi:10.29083/HJ.46.03.2023/SC249.